MOLECULAR AND CELLULAR BIOLOGY, Mar. 2004, p. 1823–1835 Vol. 24, No. 5
0270-7306/04/$08.00+0 DOI: 10.1128/MCB.24.5.1823–1835.2004

ATM and the Catalytic Subunit of DNA-Dependent Protein Kinase Activate NF-κB through a Common MEK/Extracellular Signal-Regulated Kinase/p90^{rsk} Signaling Pathway in Response to Distinct Forms of DNA Damage

Ganesh R. Panta,[1] Swayamjot Kaur,[1] Lakita G. Cavin,[1] Maria L. Cortés,[2] Frank Mercurio,[3] Leonard Lothstein,[1] Trevor W. Sweatman,[1] Mervyn Israel,[1] and Marcello Arsura[1]*

Department of Pharmacology, Center for Anticancer Drug Research, University of Tennessee Cancer Institute, College of Medicine, Memphis, Tennessee 38163[1]; Molecular Neurogenetics Unit, Department of Neurology, Massachusetts General Hospital, Harvard Medical School, Charlestown, Massachusetts 02129[2]; and Celgene Signal Research Division, San Diego, California 92121[3]

Received 2 July 2003/Returned for modification 21 August 2003/Accepted 2 December 2003

We have identified a novel pathway of ataxia telangiectasia mutated (ATM) and DNA-dependent protein kinase (DNA-PK) signaling that results in nuclear factor κB (NF-κB) activation and chemoresistance in response to DNA damage. We show that the anthracycline doxorubicin (DOX) and its congener *N*-benzyladriamycin (AD 288) selectively activate ATM and DNA-PK, respectively. Both ATM and DNA-PK promote sequential activation of the mitogen-activated protein kinase (MAPK)/p90^{rsk} signaling cascade in a p53-independent fashion. In turn, p90^{rsk} interacts with the IκB kinase 2 (IKK-2) catalytic subunit of IKK, thereby inducing NF-κB activity and cell survival. Collectively, our findings suggest that distinct members of the phosphatidylinositol kinase family activate a common prosurvival MAPK/IKK/NF-κB pathway that opposes the apoptotic response following DNA damage.

Resistance to cancer chemotherapy may be achieved in multiple ways. In addition to transmembrane-mediated export mechanisms, the disruption of the apoptotic pathways initiated by antineoplastic drugs may lead to chemoresistance (30, 40). Recent evidence indicates that an additional pathway involved in inducible chemoresistance is triggered by anticancer drug-mediated activation of the NF-κB transcription factor, which potently inhibits the apoptotic response following DNA damage (31). Typically, activation of NF-κB involves its release from an IκB molecule in the cytoplasm and translocation to the nucleus. In response to DNA double-strand breaks (DSBs) generated by topoisomerase (topo) I and II poisons, IκB-α is phosphorylated at Ser32 and Ser36 by the IκB kinase (IKK) complex (6, 10, 15, 37), which is formed by the IKK-1 and IKK-2 catalytic subunits and by a scaffold subunit termed IKK-γ/NEMO (32). As a consequence of phosphorylation, the IκB-α protein is rapidly ubiquitinated on lysine residues 21 and 22 and degraded through the proteasome pathway, thereby allowing for migration of NF-κB to the nucleus, where it regulates the expression of a variety of genes involved in cell survival (6, 52). Consistent with this mechanism, inhibition of NF-κB activity through ectopic expression of a degradation-resistant mutant IκB-α sensitized chemoresistant tumors to the topo I poison camptothecin (CPT) (51).

Although the prosurvival role of NF-κB in response to anticancer drug treatment has been well documented, the mechanism of NF-κB activation upon drug- or irradiation (IR)-induced DNA DSBs remains poorly understood. Previously, two independent studies have reported an essential role of the ataxia telangiectasia (A-T) mutated (ATM) gene during NF-κB activation following IR or CPT-induced DSBs (24, 38). Furthermore, activation of the IKK complex upon IR or neocarzinostatin treatment was found to be severely impaired in A-T lymphoblasts, suggesting that IKKs are required for ATM-mediated induction of NF-κB in response to DNA DSBs (26).

ATM is a nuclear serine-threonine kinase that belongs to the family of phosphatidylinositol kinase (PIK)-related kinases, which, following DNA DSBs, activate multiple pathways involved in stress response, cell cycle progression, and DNA DSB repair (17, 47). For example, in response to DNA damage, ATM regulates p53 transcriptional activity through direct phosphorylation on serine 15 and promotes p53 stabilization through phosphorylation of Chk2 and Mdm2 (47). Importantly, in gamma-irradiated A-T cells, defective activation of MAP kinases (MAPKs), including extracellular signal-regulated kinase (ERK), c-Jun N-terminal kinase (JNK), and p38γ, has been documented (18, 23, 46, 48, 53). Because the MEK/MAPK signaling pathway has been implicated in NF-κB activation in response to DNA damage (41) and oncogenic Ras transformation (1), here we tested whether ATM promoted NF-κB activation through MEK/ERK in response to drug-induced DNA damage.

We show that, in response to doxorubicin (DOX)-induced DNA DSBs, ATM activates a p53-independent MEK/ERK/p90^{rsk}/IKK signaling pathway that leads to NF-κB activation and cell survival. Importantly, we report that the catalytic subunit of DNA-dependent protein kinase (DNA-PKcs), but not ATM, mediates NF-κB activation via the same MEK-to-IKK

* Corresponding author. Mailing address: Department of Pharmacology, University of Tennessee College of Medicine, 874 Union Ave., Memphis, TN 38163. Phone: (901) 448-1733. Fax: (901) 448-7206. E-mail: marsura@utmem.edu.

signaling pathway in response to treatment with the catalytic inhibitor of topo II *N*-benzyladriamycin (AD 288).

Overall, our findings suggest that PIK-related kinases can activate both proapoptotic (p53 and JNK) and antiapoptotic (IKK) pathways through common upstream mediators and that the balance between these opposing signals modulates the cellular response to DNA damage.

MATERIALS AND METHODS

Cell culture and treatment conditions. Murine embryo fibroblasts (10)1 (14) and NIH 3T3 RelA and 3T3 RelA$^{-/-}$ (5) were grown in high-glucose Dulbecco's modified Eagle medium (DMEM; BioWhittaker, Walkersville, Md.) with 10% fetal bovine serum (FBS; Gibco/BRL, Rockville, Md.). (10)1 val cells express a temperature-sensitive mutant p53 and were described previously (55). HEK 293 cells were grown in RPMI medium (Cellgro, Herndon, Va.) with 10% FBS. Simian virus 40-transformed human fibroblast lines from a healthy A-T heterozygote (GM00637) and a patient with A-T (GM09607) were obtained from Coriell Cell Repositories (Camden, N.J.) and grown at low passage in Eagle minimal essential medium plus Earle salt (Sigma, St. Louis, Mo.) with 15% FBS. V-3F18 (gift from D. J. Chen, Lawrence Berkeley National Laboratory, Berkeley, Calif.), AA8, and V-3 cells (8) were grown in high-glucose DMEM with 10% FBS and 94 μM β-mercaptoethanol.

Cells were incubated with either 5 μM DOX (Sigma), 5 μM AD 288 (29) dissolved in dimethyl sulfoxide (DMSO), carrier DMSO as a control, or 20 ng of tumor necrosis factor alpha (TNF-α; Sigma)/ml. For treatment, cells were also incubated for periods of time specified below with 50 to 100 μM PD98059, 10 to 20 μM UO126, 5 mM caffeine, 50 nM to 5 μM wortmannin, and 20 μM MG132, all from Calbiochem (San Diego, Calif.), and 2 μg of cycloheximide (CHX; Sigma)/ml. Cells were irradiated with 80 Gy with a MARK I gamma irradiator.

Transfection conditions. For transient transfection, HEK 293 and GM09607 cells were plated at low confluence in 96-well plates and transfected in triplicate with a solution of DNA and Lipofectamine reagent according to manufacturer's instructions (Gibco/BRL). Sixteen hours after transfection, cells were treated with 5 μM DOX or DMSO carrier solution for 5 h. Cells were harvested after treatment according to the manufacturer's protocol in the dual-luciferase reporter assay system (Promega, Madison, Wis.), and lysates were analyzed with a Labsystems Luminoskan 96-well plate luminometer (Thermolab Systems, Needham Heights, Mass.). Firefly luciferase activity was normalized for *Renilla* luciferase activity, and results were expressed as levels of induction over vehicle-treated cells. Means and standard deviations reflect the results of at least three experiments, each carried out in triplicate.

Plasmids, small interfering RNAs (siRNAs), adenoviruses, and herpes simplex virus (HSV) amplicon vectors. The wild-type IκB-α–glutathione *S*-transferase (GST) was a generous gift from J. Hiscott (Institut Lady Davis de Recherches Medicales, Montreal, Quebec, Canada) (27). N-terminally Flag-tagged ATM (pcDNA3-Flag-ATM) and its kinase-dead mutant version (pcDNA3-Flag-KD-ATM) were kind gifts from M. Kastan (St. Jude Children's Research Hospital, Memphis, Tenn.). N-terminally hemagglutinin (HA)-tagged p90^{rsk} (pcDNA3-RSK1) and its kinase-dead mutant version (p90^{rsk}-D205N) were generous gifts from A. Zantema (Leiden Univiversity, Leiden, The Netherlands) (45). dnMEK1, the dominant negative mutant version of MEK, was a generous gift from J. Xie (University of Texas, Galveston) (54). Vectors expressing constitutively active mutant IKK-2 (IKK SS/EE) and the dominant negative mutant IKKAP1 (IKKAPΔC) have been described previously (34).

The SMARTpool siRNAs specific for p90^{rsk} and MAPK1 (ERK2) were purchased from Upstate Biotechnology (Lake Placid, N.Y.) and were lipofected into cells according to the manufacturer's specifications with Lipofectamine 2000 (Invitrogen, Carlsbad, Calif.). As a negative control, we employed four pooled nonspecific siRNA duplexes that were purchased from Upstate.

The adenovirus vectors expressing wild-type IKK-1 and IKK-2 and dominant negative forms of IKK-1 (IKK-1 K>M) and IKK-2 (IKK-2 K>M) have been described previously (2). Virus stocks were amplified to high titer (Quantum Biotechnologies, Montreal, Canada). The concentration of viral particles was determined as described previously (2).

The basic amplicon vector HGCX, containing a reporter cassette consisting of the enhanced green fluorescent protein (EGFP) gene under the control of the HSV type 1 (HSV-1) immediate-early promoter, IE4/5, has been previously described (42). The HSV-1 amplicon vector carrying the full-length cDNA encoding NH_2-terminal Flag-tagged wild-type ATM (pHGC-ATM) was obtained by subcloning the Flag-ATM into the HGCX amplicon under the control of the cytomegalovirus promoter (9). The efficiency of gene delivery was determined as described previously (9).

Electrophoretic mobility shift assay (EMSA). Nuclear extracts were prepared as described previously (1). Protein concentration was determined with the Bio-Rad Laboratories (Hercules, Calif.) protein assay. The sequences of the URE-κB- and Octamer-1 (Oct-1)-containing oligonucleotides are 5′-AAGT CCGGGTTTTCCCCAACC-3′ and 5′-TGTCGAATGCAAATCACTAGAA-3′, respectively.

EMSA was performed as described previously (1) using approximately 2 ng of labeled oligonucleotide (20,000 dpm) and 5 μg of nuclear extract, and complexes were resolved in 4.5% polyacrylamide gels.

Immunoblot analysis and IKK kinase assay. For isolation of whole-cell extracts (WCEs), cells were resuspended in cold PD buffer (40 mM Tris [pH 8], 500 mM NaCl, 6 mM EDTA, 6 mM EGTA, 10 mM glycerophosphate, 10 mM NaF, 10 mM *p*-nitrophenyl phosphate, 300 μM Na_3V0_4, 1 mM benzamidine, 2 μM phenylmethylsulfonyl fluoride, 1 mM dithiothreitol, 1 μg of leupeptin/ml, 10 μg of aprotinin/ml, 1 μg of pepstatin/ml, and 0.5% NP-40), sonicated briefly, and incubated at room temperature for 30 min. Extracts were then cleared by centrifugation at 40,000 rpm (Beckman TLA-100.3 fixed-angle rotor) for 30 min at 4°C. The IKK and p90^{rsk} kinase assay was performed using GST–IκB-α or GST–IKK-2 as described previously (1). Samples (20 to 40 μg) were subjected to electrophoresis on a sodium dodecyl sulfate–10% polyacrylamide gel, and immunoblotting was performed as previously described (3). The antibody preparations for IκB-α (sc-371), IKK-1 and -2 (sc-7607), ERK (Sc-93-G), phospho-ERK (E-4), actin (sc-1615), ribosomal S6 kinase (sc-231), and HA (sc-805) were purchased from Santa Cruz Biotechnology, Inc. (Santa Cruz, Calif.). The anti-Flag (F4042) and anti-phospho-MEK1 and -2 (M7683) antibodies were purchased from Sigma. The anti-rabbit immunoglobulin G (IgG; 12-370) was purchased from Upstate Biotechnology. The antibody preparations against ATM (MS-ATM10-PX1) and phospho-ATM (pS1981) were purchased from GeneTex (San Antonio, Tex.) and Rockland (Gilbertsville, Pa.), respectively. The antibody preparation specific for phospho-IKK-1 and -IKK-2 was obtained from Cell Signaling Technology Inc. (Beverly, Mass.).

RESULTS

Activation of the prosurvival IKK/NF-κB signaling pathway by anthracyclines is independent of p53 and DNA DSBs. Because ectopic expression of p53 has been shown to promote activation of NF-κB (41), we sought to determine whether NF-κB activation by DNA-damaging agents would be impaired in p53 null cells. Surprisingly, EMSA of p53 null 10(1) cells treated with 5 μM DOX showed an activation of NF-κB DNA binding activity at the 3-h time point that remained elevated up to 12 h (Fig. 1A, left). Next, we assessed NF-κB activation by the anthracycline congener AD 288, which inhibits topo II without causing DNA DSBs (28). (10)1 cells treated with 5 μM AD 288 displayed a more pronounced induction of NF-κB DNA binding activity at the 3-h time point than DOX-treated cells, and induction started to decrease at the 12-h time point (Fig. 1A, right). Similar results were obtained with DOX- or AD 288-treated p53 null SAOS cells (data not shown). Thus, p53 activity is not required for NF-κB activation by topo II inhibitors. In addition, NF-κB can be activated in response to catalytic inhibition of topo II independent of DNA DSBs.

Because the slow kinetics of activation of NF-κB by DOX suggested that activation might require prior protein synthesis, we assessed the levels of NF-κB activity in (10)1 cells treated in the presence or absence of the protein synthesis inhibitor CHX (2 μg/ml) for 10 min, followed by treatment with 5 μM DOX for 3 h. CHX or DOX treatment alone led to an approximately fivefold induction of NF-κB DNA binding activity (Fig. 1B). Importantly, treatment with CHX plus DOX resulted in an eightfold induction of NF-κB activity. Thus, these data rule out the possibility that a cytokine secreted in response to DNA damage mediates NF-κB activation.

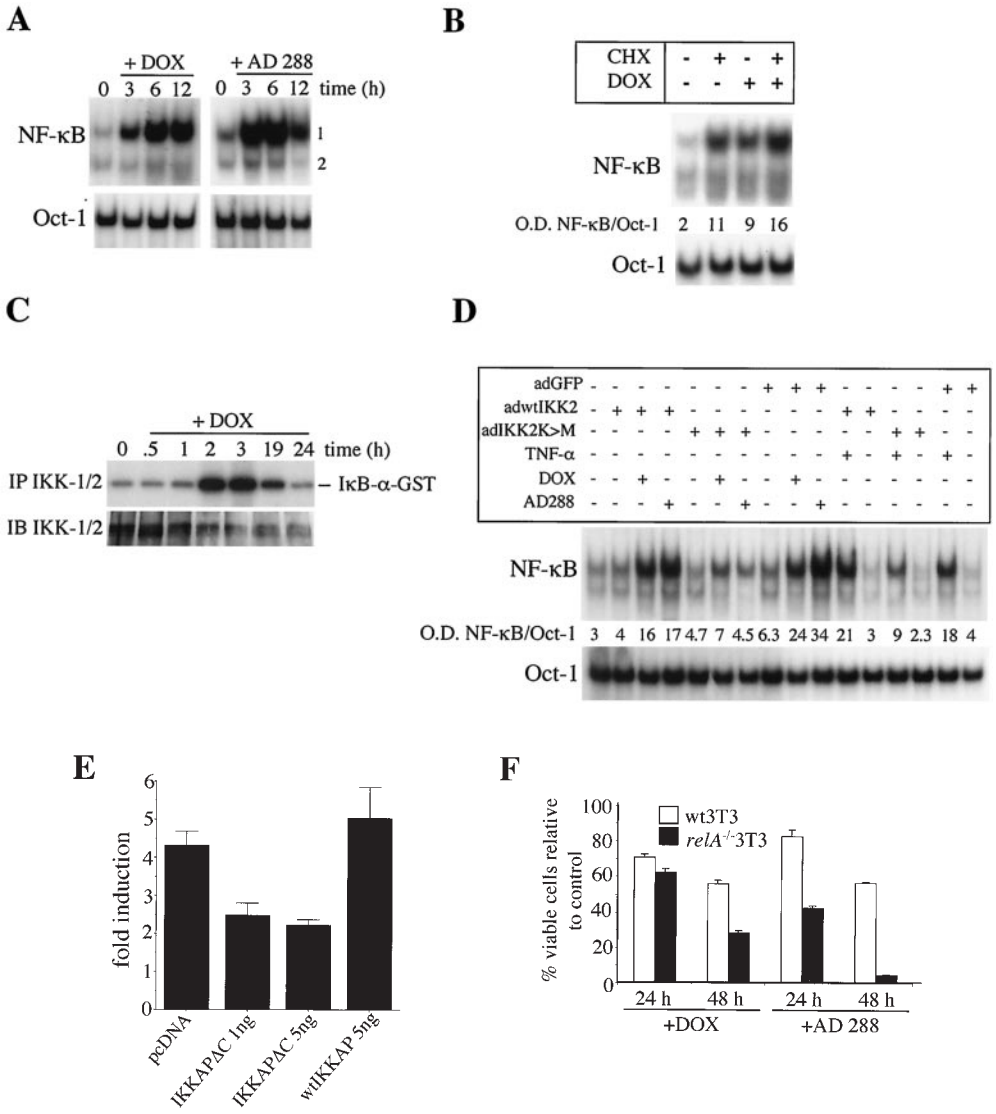

FIG. 1. The IKK complex mediates NF-κB activation and cell survival in response to anthracycline treatment. (A) P53 null (10)1 murine embryo fibroblasts were treated for the indicated times with 5 μM DOX or 5 μM AD 288. To measure the levels of NF-κB binding activity, nuclear extracts (5 μg) were subjected to EMSA using the upstream NF-κB element from the c-*myc* gene (URE-κB) as a probe (11). Band 1, classical NF-κB (p65/p50); band 2, p50 homodimers. As control for equal loading, EMSA was also performed with an Octamer-1 (Oct-1) probe. (B) (10)1 cells were treated for 10 min with 2 μg of CHX/ml, followed by incubation for 3 h in the presence or absence of DOX (5 μM). Nuclear extracts (5 μg) were subjected to EMSA as described above. Bands were quantified by densitometric analysis and are expressed as the ratios of the optical density (O.D.) of NF-κB to that of Oct-1. (C) (10)1 cells were treated for the indicated times with 5 μM DOX, and WCEs were isolated in kinase buffer. WCEs were immunoprecipitated (IP) with antibodies against IKK-1 and -2, and an aliquot was subjected to a kinase assay using IκB-α–GST as the substrate (top). An equal aliquot of each immunoprecipitant was subjected to immunoblotting (IB) as indicated (bottom). (D) (10)1 cells were infected with 10 PFU of adenovirus constructs directing expression of wild-type (wt) IKK-2 or IKK-2 K>M for 24 h. Subsequently, cells were treated for 5 h with 5 μM DOX, 5 μM AD 288, or DMSO carrier solution. Alternatively, cells were treated for 30 min with 20 ng of TNF-α/ml or bovine serum albumin carrier solution. Nuclear extracts (5 μg) were subjected to EMSA using as a probe the URE-κβ or the Oct-1 oligonucleotide. (E) HEK 293 cells were plated in triplicate in 96-well plates and transfected by lipofection with 50 ng of NF-κB–luciferase construct in the presence of the indicated amount of wtIKKAP or IKKAPΔC expression vectors and, as an internal control, a *Renilla* luciferase expression plasmid. Total DNA concentration was adjusted to 150 ng with backbone vector (pcDNA). Following 24 h of treatment with 5 μM DOX, luciferase activity was measured and expressed as induction relative to that of DMSO-treated cells, which was set at 1. Means and standard deviations are representative of three independent experiments carried out in triplicate. (F) Cultures of wild-type and RelA null NIH 3T3 cells were incubated in medium containing 5 μM DOX, 5 μM AD 288, or DMSO carrier solution for 24 and 48 h. Cell proliferation was monitored by conversion of MTS to its formazan product. Means and standard deviations are representative of three independent experiments carried out in triplicate.

To assess the ability of IKK-1 and IKK-2 to phosphorylate IκB-α in response to DOX and AD 288 treatment, we carried out a kinase assay using GST–wild-type IκB-α fusion proteins. Extracts were prepared from DOX-treated (10)1 cells, immunoprecipitated with antibodies against IKK-1 and -2, and subjected to kinase assays as described previously (1). We detected maximal induction of IKK kinase activity after 2 to 3 h of DOX treatment (Fig. 1C), which indicates conformity with the kinet-

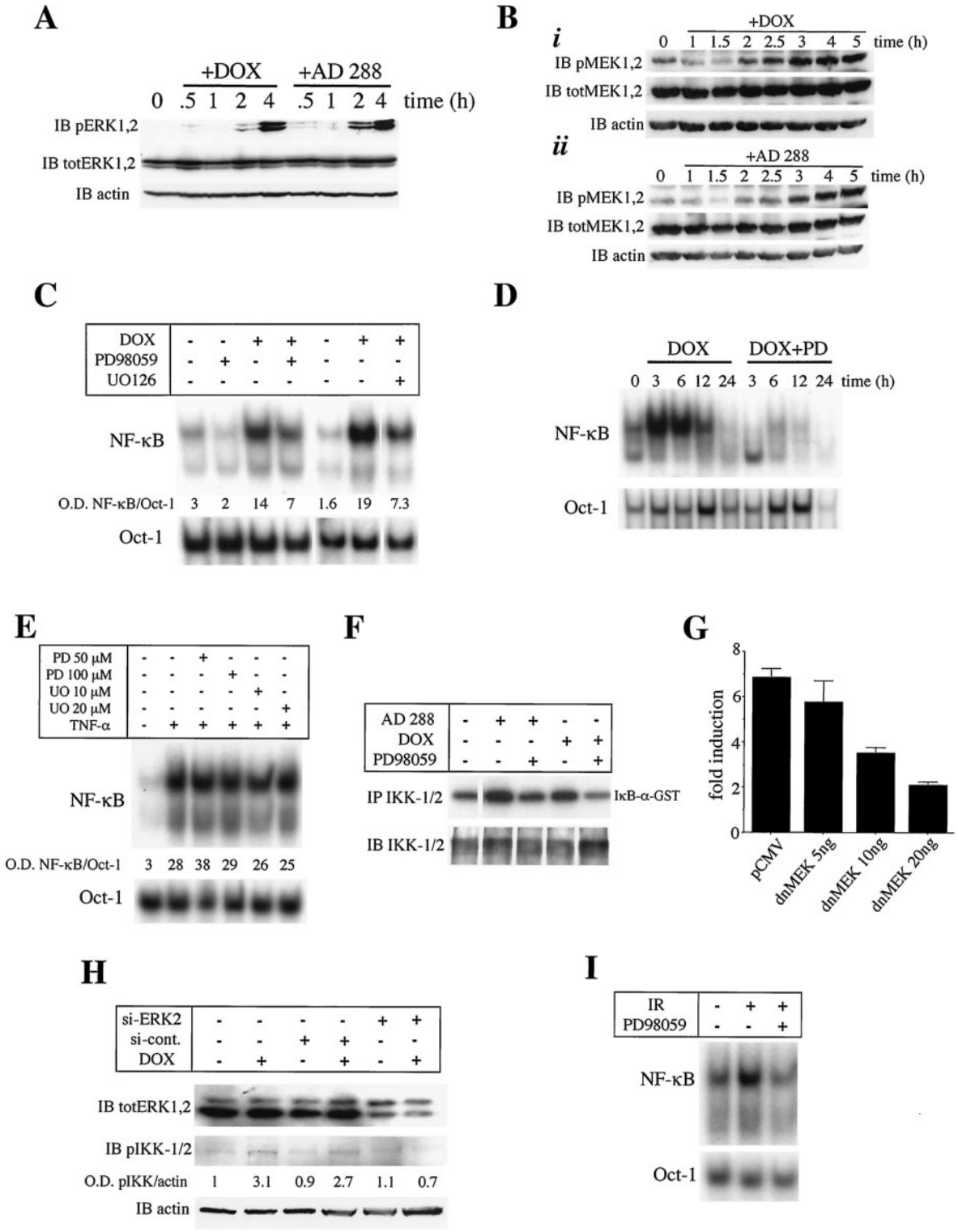

FIG. 2. The MEK/ERK signaling pathway mediates NF-κB activation by DOX and AD 288. (A and B) Serum-starved (10)1 cells were treated for the indicated times with 5 μM DOX or 5 μM AD 288. WCEs (40 μg) were subjected to immunoblotting (IB) using a phospho-specific ERK antibody (pERK1,2), an antibody against phospho-MEK (S218/S222; pMEK1,2), or antibodies that recognize total ERKs (totERK1,2) or total MEKs (totMEK1,2). For equal loading, the same filters were hybridized with an antibody against actin. (C) (10)1 cells were treated for 5 h with 5 μM DOX or 5 μM AD 288 with or without PD98059 (50 μM) or UO126 (20 μM). Nuclear extracts (5 μg) were subjected to EMSA using the URE-κB or Oct-1 probes. O.D., optical density. (D) (10)1 val cells were treated at the nonpermissive temperature of 39°C for the indicated times with 5 μM DOX in the presence or absence of PD98059 (100 μM). Nuclear extracts (5 μg) were subjected to EMSA as described above. (E) (10)1 val cells were treated at the nonpermissive temperature of 39°C for 1 h with 20 ng of TNF-α/ml with or without PD98059 (PD; 50 to 100 μM) or UO126 (UO; 10 to 20 μM). Nuclear extracts (5 μg) were subjected to EMSA as described above. (F) (10)1 cells were treated for 2 h with 5 μM

ics of NF-κB DNA binding activity observed previously (Fig. 1A). In contrast, we did not detect IKK kinase activity using IκB-α with mutations at serines 32 and 36 (data not shown). Thus, the IKK complex mediates IκB-α phosphorylation in response to AD 288 and DOX treatment.

To further confirm these results, (10)1 cells were infected with adenovirus constructs expressing wild-type IKK-2 or the dominant negative IKK-2 K>M, a potent repressor of NF-κB activity (34). After 24 h of infection, nuclear extracts from cells treated with DOX, AD 288, or TNF-α were isolated and subjected to EMSA as described above. Cells expressing green fluorescent protein (GFP) or wild-type IKK-2 displayed increased levels of NF-κB binding in response to DOX or AD 288 treatment (Fig. 1D). In contrast, NF-κB activation by DOX or AD 288 was inhibited in cells expressing IKK-2 K>M. As expected, IKK-2 K>M, but not wild-type IKK-2, attenuated NF-κB activation in response to TNF-α treatment. Similarly, ectopic expression of the dominant negative mutant IKKAPΔC, which had been shown previously to block IKK complex activation by TNF-α and Ras (1, 33) but not that of its wild-type counterpart, wt IKKAP, inhibited DOX- and AD288-mediated induction of NF-κB luciferase activity (Fig. 1D). Thus, activation of the IKK complex is required for induction of NF-κB by anthracycline congeners.

To determine the role of NF-κB during anthracycline-mediated cell killing, cultures of wild-type and p65 (RelA) null NIH 3T3 cells were incubated in the presence of DOX, AD 288, or DMSO carrier alone for 24 and 48 h and cell viability was monitored by MTS assay. DOX or AD288 treatment for 48 h resulted in approximately 40% cell death of wild-type NIH 3T3 cells. Interestingly, similarly treated RelA null cells displayed 75 and 95% cell death, respectively (Fig. 1F). Furthermore, ectopic expression of RelA in RelA null NIH 3T3 cells rescued cell killing by DOX (data not shown). Thus, the results from this genetic analysis support a model in which inhibition of NF-κB activity potentiates anthracycline-mediated cell killing.

A p53-independent MEK/ERK signaling pathway mediates IKK complex and NF-κB activation in response to anthracycline treatment. MAPKs have been implicated in NF-κB activation in response to Ras activation (1, 13, 45, 50) or ectopic expression of p53 (41). Thus, we sought to determine whether anthracycline drug treatment also promoted activation of NF-κB through the MEK/ERK signaling pathway. Indeed, we detected induction of ERK and MEK phosphorylation after 2 h of DOX or AD 288 treatment (Fig. 2A and B). Consistent with our previous results in Fig. 1B, CHX treatment did not prevent induction of ERK phosphorylation by DOX or AD 288 (data not shown), excluding the possibility that the autocrine secretion of a cytokine in response to DNA damage promoted MAPK activation.

Given the coordinated induction of ERK phosphorylation and NF-κB DNA binding activity in response to either DOX or AD 288 treatment, we sought to determine the effects of inhibition of MEK on NF-κB activation. Treatment of (10)1 cells with the MEK inhibitors PD98059 and UO126 resulted in downregulation of DOX-mediated activation of NF-κB (Fig. 2C). Similar results were obtained for AD 288-treated cells (data not shown). Likewise, PD98059 treatment of (10)1 val cells at the nonpermissive temperature led to complete inhibition of NF-κB induction by DOX (Fig. 2D). Importantly, treatment with 50 to 100 μM PD98059 or 10 to 20 μM UO126 did not inhibit the activation of NF-κB elicited by TNF-α treatment (Fig. 2E), indicating that these compounds selectively target the MEK/ERK/NF-κB pathway at these concentrations. As predicted by our previous results, DOX- and AD 288-mediated induction of endogenous IKK-1 and IKK-2 kinase activity was inhibited by PD98059 treatment (Fig. 2F). Furthermore, ectopic expression of a dominant negative mutant MEK (54) in HEK 293 cells reduced DOX-mediated induction of an NF-κB-driven luciferase construct in a dose-dependent manner (Fig. 2G).

To further assess the role of ERKs during activation of NF-κB in response to DOX treatment, we used RNA interference to disrupt ERK2 gene expression and measured the levels of activation of the IKK complex in response to DOX treatment. For this purpose, we used an antibody specific for the phosphorylated forms of IKK-1 and IKK-2 raised against serines 180 and 181, respectively, within their activation loop. We detected a significant enhancement of IKK phosphorylation levels following 2 h of DOX in untreated or siRNA control-treated cells. In contrast, silencing the expression of ERK2 attenuated the phosphorylation levels of the IKK complex following DOX treatment (Fig. 2H). Thus, ERK2 is required for DOX-mediated activation of NF-κB.

We next determined the levels of NF-κB activity in gamma-irradiated cells treated in the presence or absence of PD98059. Exposure of (10)1 cells to 80 Gy, a dose that has been previously shown to induce NF-κB activity (16), resulted in upregulation of NF-κB DNA binding levels, which was inhibited by pretreatment with PD98059 (Fig. 2I). Thus, the MEK/ERK pathway mediates NF-κB activation in response to another DNA DSB-inducing agent.

In conclusion, the results from the EMSA, kinase assay, transient transfection, and RNA interference assay indicate an

DOX or 5 μM AD 288 with or without PD98059 (100 μM). The IκB kinase assay was performed as described in the legend of Fig. 1. (G) HEK 293 cells were plated in triplicate in 96-well plates and transfected by lipofection with 50 ng of the NF-κB–luciferase construct in the presence of the indicated amount of dominant negative (dn) MEK expression vector and, as an internal control, a *Renilla* luciferase expression plasmid. The final DNA concentration was adjusted to 150 ng with the parental control vector pCMV. Following 24 h of treatment with 5 μM DOX, luciferase activity was determined as described in the legend of Fig. 1. Means and standard deviations (bars) are representative of three independent experiments carried out in triplicate. (H) HEK 293 cells were lipofected with 100 nM siRNA specific for ERK2 (si-ERK2) or 100 nM nonspecific siRNA control (si-cont). After 48 h of transfection, cells were treated for 2 h with 5 μM DOX or DMSO carrier solution and WCEs were subjected to immunoblotting with an antibody specific for ERK-1 and -2 (top) or an antibody that recognizes IKK-1 and -2 phosphorylated at serines 180 and 181, respectively (middle). The same blot was also hybridized with an antibody against actin (bottom). (I) (10)1 val cells were treated for 1 h in the presence or absence of PD98059 (50 μM). Cells were then irradiated with 80 Gy and incubated at 39°C for 3 h. Nuclear extracts (5 μg) were subjected to EMSA as described above.

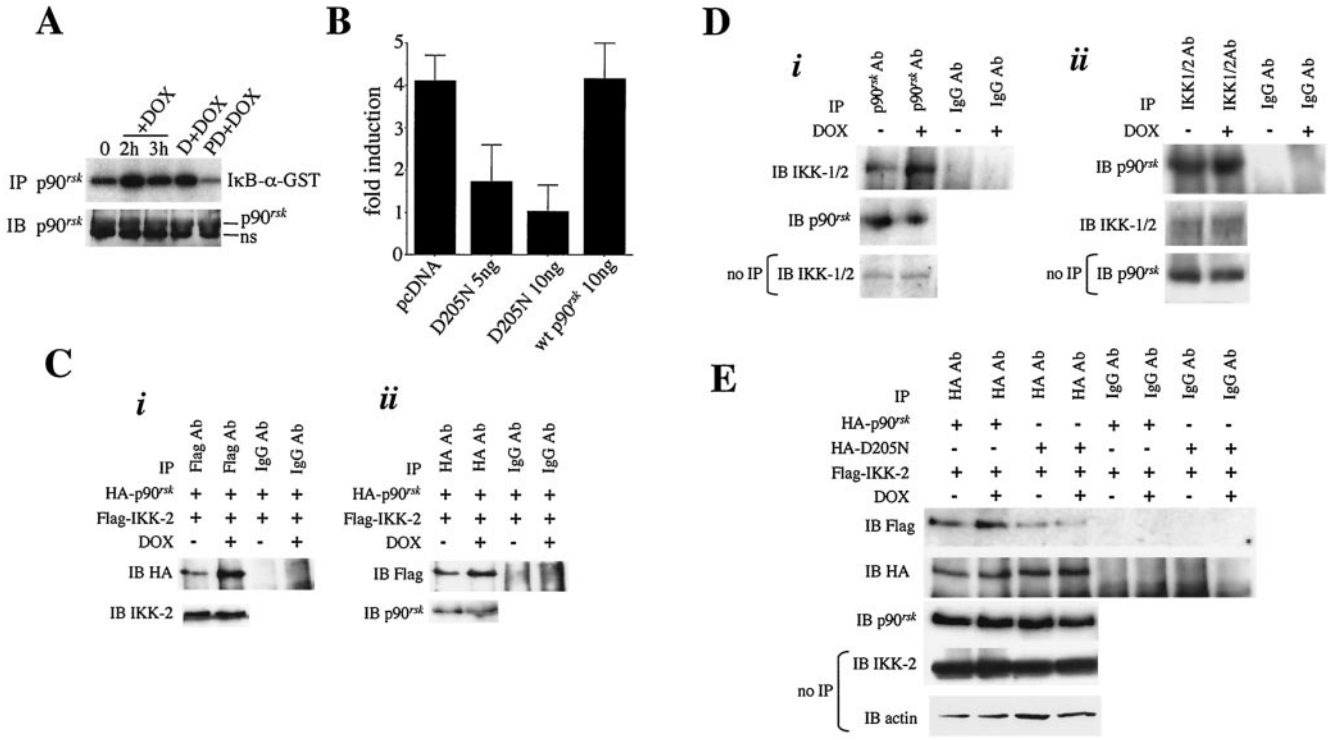

FIG. 3. p90^{rsk} mediates IKK complex and NF-κB activation by anthracyclines through association with the IKK-2 subunit. (A) (10)1 cells were treated at the indicated time points with 5 μM DOX or 5 μM AD 288 in the absence or presence of PD98059 (100 μM). Following immunoprecipitation (IP) with an antibody against p90^{rsk}, a kinase assay using IκB-α–GST as the substrate was performed (top). An equal aliquot of each immunoprecipitant was subjected to immunoblotting (IB) as indicated (bottom) with an anti-p90^{rsk} antibody. ns, nonspecific. (B) HEK 293 cells were plated in triplicate in 96-well plates and transfected by lipofection with 50 ng of NF-κB–luciferase construct in the presence of the indicated amount of empty vector (pcDNA) or vectors directing expression of either the wild-type (wt) or dominant negative (D205N) p90^{rsk} gene. Following 24 h of treatment with 5 μM DOX, luciferase activity was determined as described in the legend of Fig. 1. Means and standard deviations are representative of three independent experiments carried out in triplicate. Bars represent standard deviations. (C) HEK 293 cells were transfected by lipofection with vectors directing expression of N-terminally HA-tagged p90^{rsk} (HA-p90^{rsk}) or Flag-tagged IKK-2 (Flag–IKK-2). Transfected cells were treated for 2 h with 5 μM DOX or DMSO carrier solution. Following immunoprecipitation with an antibody (Ab) against Flag (*i*) or against HA (*ii*), immunoblotting with equal immunoprecipitated aliquots of either IKK-2 or p90^{rsk} protein, as indicated, was performed. Samples were also immunoprecipitated with an anti-IgG antibody and immunoblotted with HA or Flag as a negative control. (D) HEK 293 cells were treated for 2 h with 5 μM DOX or DMSO vehicle. WCEs (2 mg) were immunoprecipitated with an anti-p90^{rsk} antibody (*i*), an anti-IKK1 and -2 antibody (*ii*), or an anti-IgG antibody as a negative control. Following immunoprecipitation, immunoblotting of equal immunoprecipitated aliquots was performed with an anti-p90^{rsk} or an anti-IKK-2 antibody. Aliquots of nonimmunoprecipitated (no IP) WCEs (80 μg) were also subjected to immunoblotting with an anti-IKK-2 or anti p90^{rsk} antibody (bottom). (E) HEK 293 cells were transfected as described above with vectors directing expression of HA-p90^{rsk} or dominant negative mutant (HA-D205N) p90^{rsk} and Flag-tagged IKK-2 (Flag–IKK-2). Immunoprecipitation and immunoblotting were performed as described above. In addition, nonimmunoprecipitated WCEs (25 μg) were subjected to immunoblotting with antibodies against IKK-2 or actin (bottom).

essential role of the MEK/ERK signaling pathway during NF-κB activation by DNA-damaging agents.

Inducible association of p90^{rsk} and IKK-2 mediates NF-κB activation in response to DOX treatment. Given the ability of ribosomal S6 kinase (p90^{rsk}), a downstream target of ERK, to mediate NF-κB activation in response to phorbol ester treatment (12, 50), we sought to determine its role during anthracycline-mediated activation of NF-κB. To address this issue, WCEs of untreated or DOX-treated (10)1 cells were isolated, immunoprecipitated with antibodies against p90^{rsk}, and subjected to kinase assays using GST–wild-type IκB-α fusion proteins. As depicted in Fig. 3A, immunoprecipitated p90^{rsk} from DOX-treated cells displayed three- to fourfold induction of IκB-α kinase activity over control values. Consistent with our previous data, IκB-α phosphorylation by p90^{rsk} activity was inhibited by treatment with PD98059 (Fig. 3A). To assess the functional relevance of p90^{rsk} IκB-α kinase activity, we next determined the effects of ectopic expression of a dominant negative mutant p90^{rsk} (p90^{rsk}-D205N) on DOX-mediated NF-κB activation in HEK 293 cells. In p90^{rsk}-D205N, the aspartic acid at position 205 in the ATP-binding site of the amino-terminal kinase domain is replaced by asparagine (45). Expression of p90^{rsk}-D205N, but not of its wild-type counterpart, abolished DOX-mediated transcriptional activation of NF-κB (Fig. 3B). Thus, both IKK and p90^{rsk} kinase activities are required for efficient NF-κB activation in response to anthracycline treatment.

To examine whether IKKs and p90^{rsk} form a complex in vivo, we transfected an expression vector for N-terminally HA-tagged p90^{rsk} into HEK 293 cells, together with an expression vector for Flag-tagged IKK-2. After 24 h of transfection, cells were incubated for 2 h with DMSO alone or DOX. Subse-

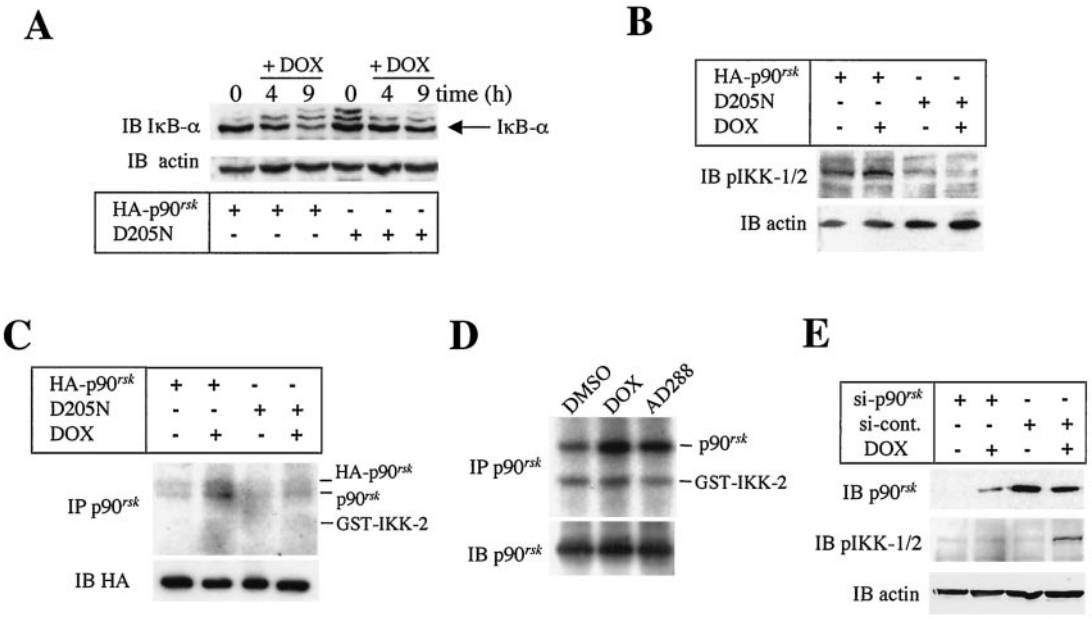

FIG. 4. p90^{rsk} is required for NF-κB activation. (A) HEK 293 cells were lipofected as described in the legend of Fig. 3 with vectors directing expression of HA-p90^{rsk} or dominant negative mutant (HA-D205N) p90^{rsk}. Transfected cells were then treated for the indicated times with 5 μM DOX. WCEs (50 μg) were subjected to immunoblotting (IB) with an anti-IκB-α or actin antibody. (B) HEK 293 cells were transfected as described above and treated for 2 h with 5 μM DOX. WCEs were subjected to immunoblotting with an antibody that recognizes IKK-1 and -2 phosphorylated at serines 180 and 181, respectively (top). The same blot was also hybridized with an antibody against actin (bottom). (C) HEK 293 cells were transfected by lipofection with vectors directing expression of HA-tagged wild-type p90^{rsk} (HA-p90^{rsk}) or the dominant negative mutant (HA-D205N) p90^{rsk}. After 24 h, transfected cells were treated for 2 h with 5 μM DOX or DMSO carrier solution. Following immunoprecipitation (IP) with an antibody against p90^{rsk}, a kinase assay using GST–IKK-2 as the substrate was performed (top). The immunoprecipitants were also subjected to immunoblotting with the anti-HA antibody (bottom). (D) WCEs of HEK 293 cells that had been incubated for 2 h with 5 mM DOX, AD 288, or DMSO carrier solution were immunoprecipitated with an antibody specific for p90^{rsk}. Subsequently, immunoprecipitants were subjected to kinase assay as described above. Equal aliquots of the immunoprecipitants were subjected to immunoblotting with an anti-p90^{rsk} antibody. (E) HEK 293 cells were lipofected with 100 nM siRNA specific for p90^{rsk} (si-p90^{rsk}) or 100 nM siRNA nonspecific siRNA control (si-cont). After 48 h of transfection, cells were treated for 2 h with 5 μM DOX or DMSO carrier solution and WCEs were subjected to immunoblotting with a p90^{rsk}-specific antibody (top), a phospho-specific IKK-1 and -2 antibody (middle), or an antibody against actin (bottom).

quently, WCEs were immunoprecipitated with an anti-Flag antibody and immunoblotted with an anti-HA antibody. Immunoprecipitation of Flag–IKK-2 with the anti-Flag but not the anti-IgG antibody resulted in coprecipitation of HA-p90^{rsk} (Fig. 3C, *i*). Interestingly, the interaction between HA-p90^{rsk} and Flag–IKK-2 increased approximately threefold in response to DOX treatment. Similar results were obtained when WCEs were immunoprecipitated with an anti-HA antibody (Fig. 3C, *ii*). Thus, p90^{rsk} can associate with the IKK complex and this interaction is induced following DOX treatment.

To assess whether endogenous p90^{rsk} and IKK-2 proteins form a complex in vivo following DOX stimulation, we immunoprecipitated WCEs of (10)1 cells treated for 2 h with 5 μM DOX or DMSO vehicle using an anti-p90^{rsk} antibody (Fig. 3D, *i*) or an antibody specific for IKK-1 and -2 (Fig. 3D, *ii*). We detected association of IKK-2 with p90^{rsk} in DMSO-treated cells, better seen on prolonged exposure (Fig. 3D and data not shown). However, as predicted by our previous results, DOX treatment led to a significant enhancement of the interaction between p90^{rsk} and IKK-2 (Fig. 3D). Furthermore, p90^{rsk} and IKK-2 protein expression levels remained unchanged following DOX treatment (Fig. 3D), indicating that their inducible association is not simply due to augmented expression of p90^{rsk} or the IKK-2 protein. Similar results were obtained with AD 288-treated cells (data not shown). To assess whether p90^{rsk} kinase activity was required for enhanced p90^{rsk} association with the IKK complex, we transfected HA-p90^{rsk} and HA–p90^{rsk}-D205N with Flag-tagged IKK-2 in HEK 293 cells. Immunoprecipitation of HA-p90^{rsk} or HA–p90^{rsk}-D205N with the anti-HA antibody resulted in coprecipitation of Flag–IKK-2 (Fig. 3E). As we observed previously (Fig. 3D), the association between HA-p90^{rsk} and Flag–IKK-2 was increased by DOX treatment. In contrast, DOX treatment did not increase further the interaction of HA–p90^{rsk}-D205N with Flag–IKK-2. Importantly, expression of HA–p90^{rsk}-D205N did not inhibit the expression of the cotransfected wild-type IKK-2 (Fig. 3D). Thus, the inducible association between p90^{rsk} and IKK-2 is dependent on an intact ATP-binding site in the amino-terminal kinase domain of p90^{rsk}.

To determine the effect of the inducible association of p90^{rsk} with IKK-2 on IκB-α degradation, we transfected 293 cells with the HA-p90^{rsk} or the HA–p90^{rsk}-D205N construct and assessed IκB-α protein expression levels following DOX treatment. We observed a significant delay in IκB-α degradation in cells expressing HA–p90^{rsk}-D205N compared to cells transfected with the HA-p90^{rsk} vector (Fig. 4A). Consistent with the inducible association between p90^{rsk} and IKK-2 being required for IKK complex activation by DOX, cotransfection of the D205N

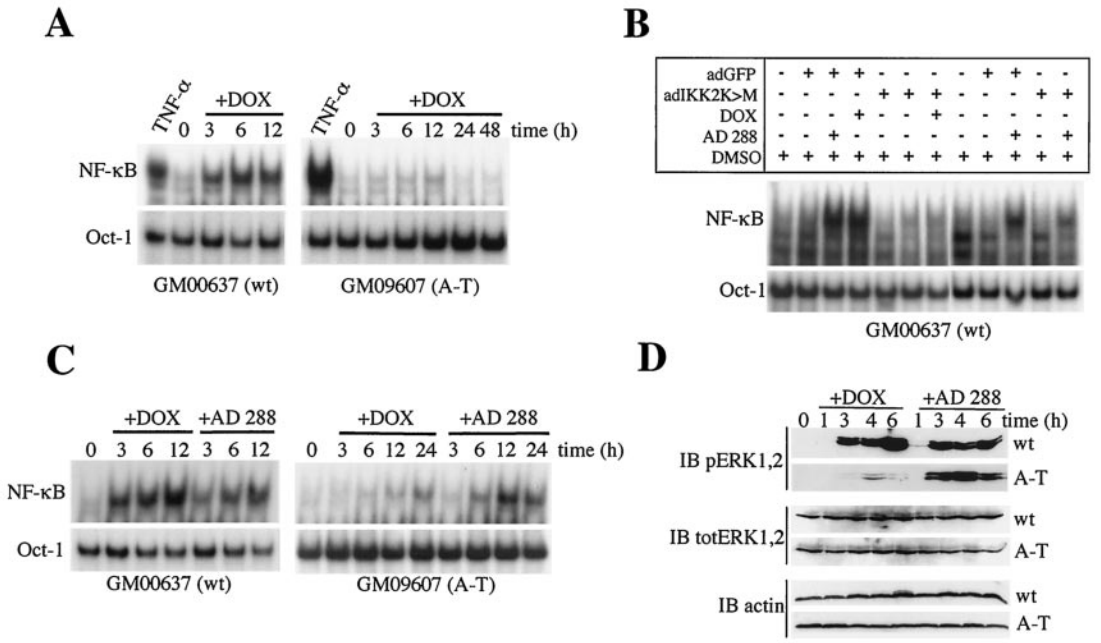

FIG. 5. ATM is required for activation of NF-κB and ERK by DOX. (A) Wild-type (GM00637) and A-T (GM09607) fibroblasts were treated for the indicated times with 5 μM DOX. Alternatively, cells were treated for 30 min with 20 ng of TNF-α/ml or bovine serum albumin carrier solution. NF-κB DNA binding activity was determined by EMSA using as probe the URE-κβ or the Oct-1 oligonucleotide, as described in the legend of Fig. 1. (B) GM00637 cells were infected for 24 h with 10 PFU of adenovirus (ad) constructs directing expression of wild-type (wt) IKK-2 or dominant negative IKK-2 K>M. Subsequently, cells were treated for 5 h with 5 μM DOX, 5 μM AD 288, or DMSO carrier solution. Nuclear extracts (5 μg) were subjected to EMSA. (C) GM00637 or GM09607 cells were treated for 5 h with 5 μM DOX, 5 μM AD 288, or DMSO carrier solution. Nuclear extracts were subjected to EMSA. (D) GM00637 (wt) or GM09607 (A-T) cells were treated for the indicated times with 5 μM DOX or 5 μM AD 288. WCEs (40 μg) were subjected to immunoblotting (IB) with an antibody that recognizes phospho-ERK species (pERK1,2) or total ERK (totERK1,2). As a control for equal loading, the same filters were hybridized with an antibody against actin.

dominant negative mutant, but not the wild-type p90^{rsk}, abolished the induction of IKK complex phosphorylation in response to DOX treatment of HEK 293 cells (Fig. 4B). To determine whether p90^{rsk} phosphorylated IKK-2 directly, aliquots of the same extract described in the legend for Fig. 4B were immunoprecipitated with an anti-HA antibody and subjected to kinase assays using GST–IKK-2 as the substrate. DOX treatment resulted in a significant induction of p90^{rsk} phosphorylation levels (Fig. 4C), presumably due to autophosphorylation. Importantly, we did not observe a significant increase of p90^{rsk}-mediated phosphorylation of GST–IKK-2 in response to DOX treatment (Fig. 4C). Consistent with this finding, we did not measure a significant phosphorylation of GST–IKK-2 by the endogenous p90^{rsk} in DOX-treated (10)1 cells (Fig. 4D). Thus, p90^{rsk} does not phosphorylate directly the IKK-2 subunit.

To provide genetic evidence of the requirement of p90^{rsk} for DOX-mediated activation of NF-κB, we used RNA interference to disrupt p90^{rsk} gene expression and measured the levels of activation of the IKK complex in response to DOX treatment. We observed a significant enhancement of IKK phosphorylation levels following 2 h of DOX in siRNA control-treated cells. In contrast, silencing the expression of p90^{rsk} attenuated the phosphorylation levels of the IKK complex following DOX treatment (Fig. 4E). Thus, p90^{rsk} is essential for DOX-mediated activation of NF-κB.

Collectively, our results indicate that inducible association between the endogenous p90^{rsk} and IKK-2 molecules is essential for anthracycline-mediated activation of NF-κB.

ATM is required for NF-κB activation in response to DOX, but not AD 288, treatment. Because Rotman and coworkers reported an essential role of the ATM gene during NF-κB activation in response to CPT and ionizing radiation (26), we sought to determine the levels of NF-κB activity in response to DOX treatment of wild-type (GM00637) and A-T (GM09607) fibroblasts (35). Treatment of GM00637 cells with 5 μM DOX for the indicated times (Fig. 5A) resulted in activation of NF-κB DNA binding activity with kinetics similar to those seen in (10)1 cells (Fig. 1A). In contrast, GM09607 fibroblasts failed to display NF-κB activation in response to DOX treatment (Fig. 5A, right). Importantly, TNF-α treatment of both cell lines resulted in efficient activation of NF-κB, indicating the specificity of the signaling impairment. Thus, ATM is required for DNA DSB-mediated induction of NF-κB activity in response to topo II (DOX) as well as topo I (CPT) poisons (26).

To further confirm the involvement of the IKK complex during anthracycline-mediated NF-κB activation, we infected wild-type fibroblasts with adenovirus constructs directing expression of IKK-2 K>M or GFP and measured NF-κB DNA binding activity following DOX or AD 288 treatment. As shown in Fig. 5B, both uninfected cells and cells expressing GFP treated for 5 h with 5 μM DOX or 5 μM AD 288 displayed increased levels of NF-κB DNA binding activity. In contrast, NF-κB activation by DOX or AD 288 in cells express-

ing IKK-2 K>M was dramatically reduced. Thus, the IKK complex is required for ATM-mediated activation of NF-κB in response to anthracycline treatment of GM00637 fibroblasts.

Next, we assessed the role of ATM during NF-κB activation in response to AD 288 treatment that does not cause DNA DSBs. Once again, DOX treatment of A-T GM09607 fibroblasts failed to activate NF-κB (Fig. 5C). In contrast, AD 288 treatment of A-T fibroblasts led to induction of NF-κB DNA binding levels to an extent comparable to that seen in their wild-type counterpart (Fig. 5C, right), indicating that ATM is dispensable for AD 288-mediated induction of NF-κB.

Because the MEK/ERK pathway is required for NF-κB activation in response to DOX treatment and ATM is essential for NF-κB activation by DOX, we sought to determine whether ERK activation by DOX in A-T fibroblasts is impaired. As shown in Fig. 5D, either DOX or AD 288 treatment of wild-type GM00637 fibroblasts led to induction of ERK phosphorylation at the 3-h time point, which indicated conformity with the kinetics of NF-κB activation seen previously (Fig. 5C). In contrast, DOX treatment of A-T fibroblasts failed to induce ERK phosphorylation (Fig. 5D), as well as NF-κB activation (Fig. 5A and C). Interestingly, AD 288 treatment of A-T fibroblasts led to efficient induction of both ERK phosphorylation (Fig. 5D) and NF-κB DNA binding activity (Fig. 5C), again indicating that AD 288 stimulates ERK and NF-κB activities through different pathways.

ATM promotes NF-κB activation through activation of the MEK/ERK signaling pathway. To further establish the role of ATM during activation of the MEK/ERK signaling pathway in response to DOX treatment, we sought to determine the effect of inhibitors of ATM kinase activity on NF-κB activation and ERK phosphorylation. For this purpose, we treated (10)1 cells with DOX or AD 288 in the presence or absence of caffeine (5 mM), which, at this concentration, has been shown to inhibit ATM and ATR kinases but not DNA-PKcs (43). As shown in Fig. 6A, caffeine reversed NF-κB activation only by DOX, not by AD 288, again suggesting that ATM and ATR do not mediate NF-κB activation in response to AD 288 treatment. Likewise, treatment of GM00637 cells with wortmannin, another well-established ATM inhibitor (4), inhibited NF-κB activation by DOX in a dose-dependent fashion (Fig. 6B), suggesting that ATM mediates NF-κB activation following DOX treatment also in GM00637 fibroblasts. As predicted by our previous data, treatment of (10)1 cells with 20 μM U0126, 5 mM caffeine, or 5 μM wortmannin reduced phosphorylation of ERK as well as activation of NF-κB following DOX treatment (Fig. 6A and C).

To demonstrate directly that ATM regulates NF-κB activation in response to DOX treatment, we infected A-T fibroblasts with the amplicon vector HGCX (expressing EGFP) or HGC-ATM (expressing EGFP and Flag-ATM), as described previously (9), and measured NF-κB DNA binding activity and ERK phosphorylation levels following DOX treatment. To assess the kinase activity of ectopic Flag-ATM, we immunoprecipitated WCEs of DOX-treated HGC-ATM-infected cells with an anti-Flag antibody. Equal aliquots of the immunoprecipitants were then subjected to immunoblot analysis using an antibody that recognizes the autophosphorylated form of ATM (4). We detected a significant induction of phosphorylated ATM at serine 1981 in response to 1 or 3 h of DOX treatment (Fig. 6D). Thus, ectopic Flag-ATM is activated in response to DOX treatment. We next assessed the levels of NF-κB and ERK activity in HGCX- and HGC-ATM-infected GM09607 (A-T) cells following DOX treatment. As shown in Fig. 6E, we did not observe induction of NF-κB DNA binding activity or enhancement of ERK phosphorylation in either uninfected cells or cells expressing GFP treated for 5 h with 5 μM DOX. In contrast, DOX-treated HGC-ATM-infected cells displayed a three- to fourfold induction of NF-κB DNA binding activity and ERK phosphorylation levels. Thus, ectopic expression of ATM is sufficient to restore both NF-κB and ERK activation by DOX in A-T cells.

To demonstrate the requirement of ATM and MEK/ERK for the induction of NF-κB transcriptional activity following DOX treatment, we transfected A-T fibroblasts with pcDNA3 mammalian vectors directing expression of N-terminally Flag-tagged ATM (pcDNA3-Flag-ATM) or its kinase-dead mutant version (pcDNA3-Flag-KD-ATM) and measured its effect on NF-κB–luciferase activity in the presence or absence of the MEK inhibitor PD98059. As expected, in A-T fibroblasts we detected only marginal activation of NF-κB–luciferase activity in response to DOX treatment (Fig. 6F). In contrast, ectopic expression of Flag-ATM resulted in an approximately sevenfold induction of NF-κB–luciferase activity following stimulation with DOX whereas ectopic expression of Flag–KD-ATM led to a more modest threefold increase of NF-κB–luciferase activity. Importantly, treatment with 50 μM PD98059 resulted in complete inhibition of DOX-mediated induction of NF-κB luciferase activity in Flag-ATM-transfected cells. Thus, ATM regulates NF-κB activation through the MEK/ERK signaling pathway.

DNA-PKcs is required for activation of the MEK/ERK signaling pathway by AD 288. Because treatment with 5 mM caffeine did not inhibit NF-κB activation by AD 288 (Fig. 6A), we asked whether another PIK-related family member was required for AD 288 activation of NF-κB. To explore this issue, we treated A-T fibroblasts with wortmannin, a broad PIK inhibitor, and assessed NF-κB DNA binding activity following incubation with AD 288 (44). Wortmannin treatment reversed NF-κB activation by AD 288 (Fig. 7A). Likewise, treatment with PD98059 or with the proteasome inhibitor MG132 inhibited the induction of NF-κB in response to AD 288 treatment (Fig. 7B), indicating that the MEK-to-IKK pathway regulates AD 288-mediated NF-κB activation also in GM09607 (A-T) cells.

Previously, it has been shown that DNA-PKcs, a member of the PIK-related family involved in DSB repair or V(D)J recombination, could be inhibited by wortmannin but was not sensitive to 5 mM caffeine treatment (44). Thus, we sought to determine whether DNA-PKcs mediates activation of NF-κB by AD 288. For this purpose, we assessed the levels of NF-κB DNA binding activity following AD 288 treatment of DNA-PKcs$^{-/-}$ cells. As shown in Fig. 7C, left, treatment of wild-type Chinese hamster ovary (CHO) AA8 cells with 5 μM AD 288 resulted in induction of NF-κB DNA binding activity with kinetics similar to those seen in GM00637 fibroblasts (Fig. 5C). In contrast, induction of NF-κB activity in AD 288-treated DNA PKcs$^{-/-}$ CHO V-3 cells was impaired (22, 36) (Fig. 7B, right). Importantly, stable expression of DNA-PKcs in the DNA-PKcs$^{-/-}$ CHO V-3F18 cells restored induction of

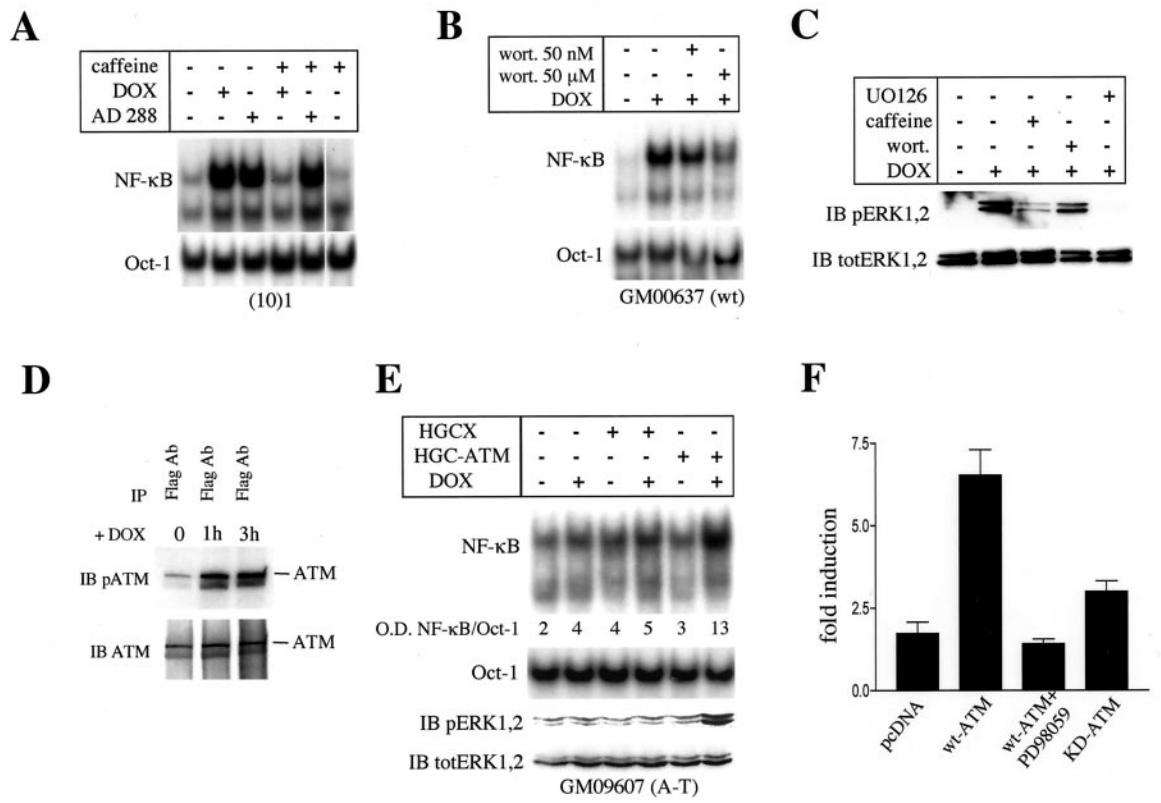

FIG. 6. ATM promotes NF-κB activation in response to DOX treatment through activation of the MEK/ERK pathway. (A) (10)1 cells were treated for 5 h with 5 μM DOX, 5 μM AD 288, or DMSO carrier solution in the absence or presence of caffeine (5 mM), and nuclear extracts were subjected to EMSA. (B) GM00637 (wild-type [wt]) cells were treated for 5 h with 5 μM DOX or DMSO carrier solution in the absence or presence of wortmannin (wort.; 50 nM or 50 μM). Nuclear extracts were subjected to EMSA. (C) (10)1 cells were treated for 5 h with 5 μM DOX or DMSO carrier solution in the absence or presence of caffeine (5 mM), wortmannin (5 μM), or UO126 (20 μM). Immunoblotting (IB) was performed with an antibody that recognizes phospho-ERK species (pERK1,2) or total ERK (totERK1,2). (D) A-T (GM09607) fibroblasts were infected at a multiplicity of infection (MOI) of 1 for 48 h with the HGC-ATM vector. Subsequently, cells were treated for the indicated times with 5 μM DOX. WCEs (800 μg) were immunoprecipitated (IP) with an anti-Flag antibody (Ab) and immunoblotted with an anti-ATM antibody or an antibody that recognizes autophosphorylated ATM at serine 1981. (E) A-T (GM09607) fibroblasts were infected at MOI of 1 for 48 h with the HGCX or the HGC-ATM vector. Subsequently, cells were treated for 5 h with 5 μM DOX or DMSO carrier solution. Nuclear extracts (5 μg) were subjected to EMSA. Alternatively WCEs (40 μg) from the same experiment were subjected to immunoblotting with an antibody that recognizes phospho-ERK species (pERK1,2) or total ERK (totERK1,2). (F) GM09607 (A-T) fibroblasts were plated in triplicate in 96-well plates and transfected by lipofection with 50 ng of the NF-κB–luciferase construct in the presence of 25 ng of pcDNA3-Flag-ATM (wt-ATM) or pcDNA3-Flag-KD-ATM (KD-ATM) expression vectors and, as an internal control, a *Renilla* luciferase expression plasmid. Total DNA concentration was adjusted to 150 ng with backbone vector (pcDNA). Following 24 h of treatment with 5 μM DOX in the absence or presence of PD98059 (50 μM), luciferase activity was measured and expressed as induction relative to that of DMSO-treated cells, which was set at 1. Means and standard deviations (bars) are representative of three independent experiments carried out in triplicate.

NF-κB DNA binding activity following AD 288 treatment (Fig. 7D). Consistent with ectopic DNA-PKcs being the mediator of NF-κB activation, treatment of CHO V-3F18 cells with PD98059 or wortmannin, but not caffeine, inhibited NF-κB activation in response to AD 288 (Fig. 7E).

Collectively, the results both from the genetic and the pharmacological analyses are consistent with a model in which DNA-PKcs is required for NF-κB activation in response to AD 288-mediated catalytic inactivation of topo II in the absence of DNA DSBs.

DISCUSSION

Here, we have identified a novel pathway of ATM signaling in response to DNA damage by anthracyclines involving sequential activation of MEK/ERK and p90^{rsk} kinase activities that results in induction of IKK/NF-κB activity and cell survival. Our findings can be summarized in the following scenario. Upon DOX treatment, MEK is phosphorylated at Ser218 and Ser222 in an ATM-dependent fashion. This event results in sequential phosphorylation of ERK and of its downstream target p90^{rsk}, which in turn associates with the IKK complex, thereby inducing IκB-α kinase activity and NF-κB activation. Remarkably, we report that DNA-PKcs, but not ATM, can activate the same MEK-to-IKK pathway in response to catalytic inhibition of topo II by AD 288 in the absence of DNA DSBs.

Previously, the ERK/MEK pathway has been implicated in NF-κB induction upon ectopic expression of p53 in SAOS cells (41). Since DOX treatment results in ATM-mediated phosphorylation of p53 and since ATM is required for NF-κB

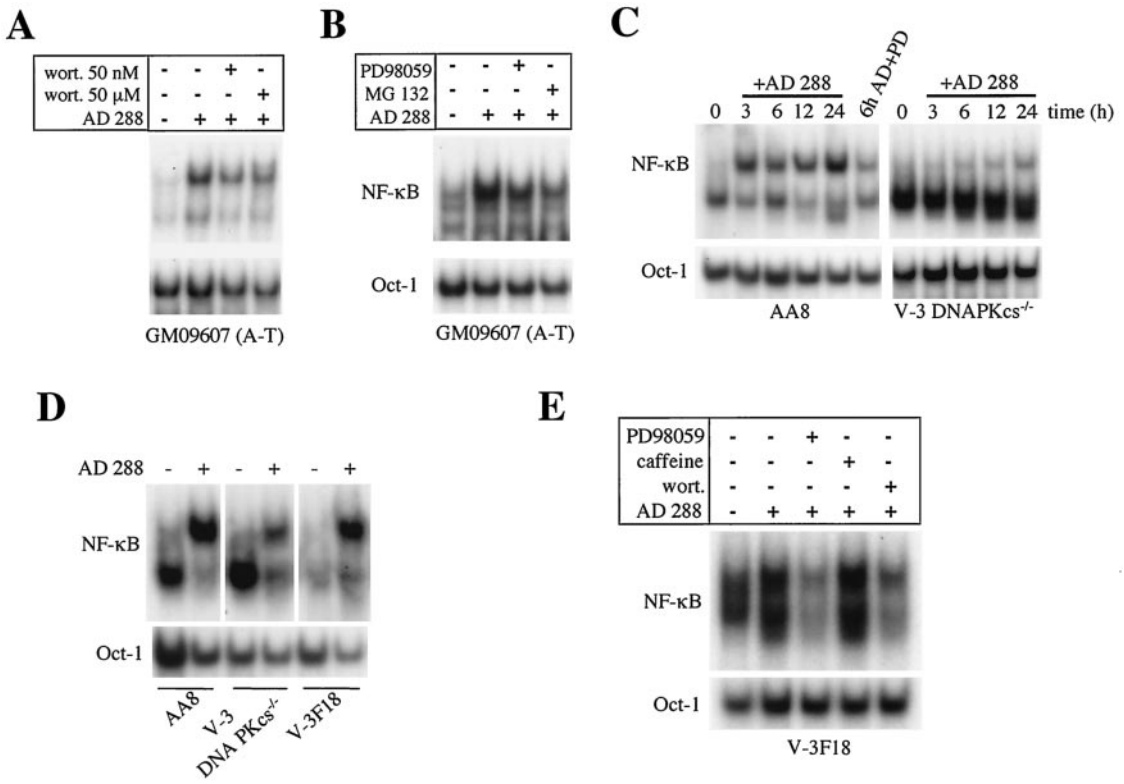

FIG. 7. DNA-PKcs mediates NF-κB activation by AD 288. (A and B) GM09607 (A-T) fibroblasts were treated for 5 h with 5 μM AD 288 or DMSO in the presence or absence of wortmannin (wort.; 50 nM or 50 μM), MG132 (30 μM), or PD98059 (50 μM), and nuclear extracts were subjected to EMSA. (C) Wild-type CHO AA8 and DNA-PKcs$^{-/-}$ CHO V-3 cells were treated with 5 μM AD 288 for the indicated times, and nuclear extracts were subjected to EMSA. PD, PD98059. (D) AA8, V-3, and V-3F18 cells that express ectopic DNA-PKcs were treated with 5 μM AD 288 for the indicated times, and nuclear extracts were subjected to EMSA. (E) V-3F18 cells were treated for 5 h with 5 μM AD 288 or DMSO in the presence or absence of wortmannin (50 nM), PD98059 (50 μM), or caffeine (5 mM), and nuclear extracts were subjected to EMSA.

activation by DNA DSBs (17), we sought to determine whether p53 activation by ATM would induce NF-κB activity through the MEK/ERK pathway. Surprisingly, we report that p53 null (10)1 cells, as well as SAOS osteoblasts (data not shown), display efficient NF-κB activation in response to DOX treatment, indicating that NF-κB activation by DOX does not rely on p53 activity. This conclusion is further supported by our data indicating that DOX treatment can induce NF-κB activity in simian virus 40-transformed GM00637 fibroblasts in which p53 is inactivated by the presence of the large T antigen (35). Although we cannot rule out the possibility that other p53-related proteins might compensate for p53 deficiency, the observation that the kinetics of NF-κB activation by DOX were not affected by the inducible expression of a temperature-sensitive p53 protein in the derivative (10)1 val cell line at the nonpermissive temperature (data not shown) strongly argues against a role for p53 during activation of NF-κB in response to DNA DSBs caused by anthracycline treatment.

Furthermore, our data together with a recent report by Tergaonkar et al., showing that IKK-1 and -2 null fibroblasts display increased cell death and p53 induction in response to DOX treatment due to downregulation of Mdm2 expression levels (49), imply that, under physiological conditions, p53 does not regulate IKK/NF-κB activity but rather lies downstream of the IKK complex.

In addition, here we have characterized the functional mechanism underlying NF-κB activation by the MEK/ERK/p90^{rsk} signaling pathway in response to anthracycline treatment. We show that disruption of this signaling pathway at multiple steps abolishes NF-κB activation by DOX or AD 288. Furthermore, we report for the first time that the ERK target p90^{rsk} associates efficiently with the IKK complex, promoting IκB-α phosphorylation and NF-κB activation. From previous data, it remained unclear how p90^{rsk}-mediated phosphorylation of IκB-α at the Ser32 residue in response to phorbol ester treatment (13, 45, 50) or Ras transformation (1, 25) would promote NF-κB activation, when efficient IκB-α degradation requires dual Ser32 and Ser36 phosphorylation (7). Here, we show that the inducible association of IKK and p90^{rsk} kinases is required for NF-κB activation by DOX. Thus, we propose that ERK-mediated phosphorylation of p90^{rsk}, which promotes enhanced interaction of p90^{rsk} with the IKK complex, is essential for NF-κB-induced chemoresistance. In this context, it will be crucial to determine whether IR-mediated activation of the ERK/p90^{rsk} pathway (19), which in this report we have shown to promote NF-κB activation, likewise induces the association between the IKK complex and the p90^{rsk} kinase.

Very recently, Hur et al. has reported that the death domain kinase RIP forms a complex with IKKs and that this interaction is essential for DOX-mediated activation of NF-κB (16).

Although neither TNF receptor signaling nor RIP kinase activity seems to play a role in this pathway, it appears that the inducible association of more than one factor with the IKK complex (e.g., $p90^{rsk}$ and RIP) is required for efficient NF-κB activation by DOX.

In addition, we report a novel mechanism of NF-κB activation by the anthracycline congener AD 288 based on sequential activation by DNA-PKcs of the downstream MEK/ERK/$p90^{rsk}$/IKK signaling pathway.

Previously, DOX has been shown to stabilize DNA/topo II complexes generating DNA DSBs (39) whereas AD 288 was found to inhibit cleavable complex formation by reducing the binding of topo II to target DNA (28). Thus, the observation that DNA-PKcs mediates NF-κB activation in response to catalytic inhibition of topo II in the absence of DNA DSBs implies that DNA-PKcs is activated in response to DNA insults through a novel mechanism distinct from DNA DSB repair or V(D)J recombination. In support of this hypothesis we did not detect phosphorylation of DNA-PKcs at Thr 2609 following AD 288 treatment (data not shown), suggesting that the mechanism of DNA-PKcs activation in response to catalytic inhibition of topo II differs from that promoted by IR (8).

Last, we have identified the MEK/ERK pathway as a novel downstream signaling pathway that is dependent on ATM kinase activity. Our findings expand a recent study by Tang et al. that reported an essential role of ATM for etoposide-mediated activation of MAPKs (48). Intriguingly, the sequence surrounding Ser218 and Ser222 within the activation loop domain of MEK does not satisfy the criteria of the ATM consensus motif (21), indicating that intermediate kinases might be responsible for phosphorylation of MEK in response to ATM activation, as shown for c-Abl during induction of the JNK/stress-activated protein kinase pathway (20). Studies to determine the mechanism of MEK activation by ATM are under way.

Overall, our findings provide the first example of selective activation by topo-interactive agents of distinct DNA damage checkpoints, which then results in the activation of the common MEK/ERK/IKK signaling pathway, resulting in cell survival. Given the ability of ATM and DNA-PK to signal cell growth arrest and apoptosis through regulation of p53 activity in response to DNA damage (17), we propose that selective activation of ATM and DNA-PKcs by DNA-damaging stimuli results in activation of common opposing signaling pathways whose relative balance determines the ultimate fate of a cell.

ACKNOWLEDGMENTS

This work was supported by the ACS grant RSG-02-255-01-TBE (M.A.) and in part by NIH grant CA78616 (M.A.). G. R. Panta was sponsored in part by the American Liver Foundation Irwin M. Arias, MD, Postdoctoral Research Fellowship. L. G. Cavin was supported by the Research Supplement for Under Represented Minorities Program, CA78616-S1. M. L. Cortés was sponsored by a fellowship from the A-T Children's Project.

We gratefully acknowledge Michael Kastan, Xandra Breakefield, Frederick Alt, John Hiscott, David Chen, Alt Zantema, Carlos Paya, David Sasson, Parker Suttle, Thomas Wirth, Amer Beg, and Jingwu Xie for kindly providing cloned DNAs and cell lines. We thank Steve Tavalin for helpful comments on the manuscript. We thank John Stuart and Mike Kaiser for the use of the gamma irradiator.

REFERENCES

1. **Arsura, M., F. Mercurio, A. L. Oliver, S. S. Thorgeirsson, and G. E. Sonenshein.** 2000. Role of the IκB kinase complex in oncogenic Ras- and Raf-mediated transformation of rat liver epithelial cells. Mol. Cell. Biol. **20:**5381–5391.
2. **Arsura, M., G. R. Panta, J. D. Bilyeu, L. G. Cavin, M. A. Sovak, A. A. Oliver, V. Factor, R. Heuchel, F. Mercurio, S. S. Thorgeirsson, and G. E. Sonenshein.** 2003. Transient activation of NF-κB through a TAK1/IKK kinase pathway by TGF-β1 inhibits AP-1/SMAD signaling and apoptosis: implications in liver tumor formation. Oncogene **22:**412–425.
3. **Arsura, M., M. Wu, and G. E. Sonenshein.** 1996. TGF β1 inhibits NF-κB/Rel activity inducing apoptosis of B cells: transcriptional activation of IκBα. Immunity **5:**31–40.
4. **Bakkenist, C. J., and M. B. Kastan.** 2003. DNA damage activates ATM through intermolecular autophosphorylation and dimer dissociation. Nature **421:**499–506.
5. **Beg, A. A., W. C. Sha, R. T. Bronson, S. Ghosh, and D. Baltimore.** 1995. Embryonic lethality and liver degeneration in mice lacking the RelA component of NF-κB. Nature **376:**167–170.
6. **Bottero, V., V. Busuttil, A. Loubat, N. Magne, J. L. Fischel, G. Milano, and J. F. Peyron.** 2001. Activation of nuclear factor κB through the IKK complex by the topoisomerase poisons SN38 and doxorubicin: a brake to apoptosis in HeLa human carcinoma cells. Cancer Res. **61:**7785–7791.
7. **Brown, K., S. Gerstberger, L. Carlson, G. Franzoso, and U. Siebenlist.** 1995. Control of IκB-α proteolysis by site-specific, signal-induced phosphorylation. Science **267:**1485–1488.
8. **Chan, D. W., B. P. Chen, S. Prithivirajsingh, A. Kurimasa, M. D. Story, J. Qin, and D. J. Chen.** 2002. Autophosphorylation of the DNA-dependent protein kinase catalytic subunit is required for rejoining of DNA double-strand breaks. Genes Dev. **16:**2333–2338.
9. **Cortes, M. L., C. J. Bakkenist, M. V. Di Maria, M. B. Kastan, and X. O. Breakefield.** 2003. HSV-1 amplicon vector-mediated expression of ATM cDNA and correction of the ataxia-telangiectasia cellular phenotype. Gene Ther. **10:**1321–1327.
10. **Das, K. C., and C. W. White.** 1997. Activation of NF-κB by antineoplastic agents. Role of protein kinase C. J. Biol. Chem. **272:**14914–14920.
11. **Duyao, M. P., A. J. Buckler, and G. E. Sonenshein.** 1990. Interaction of an NF-κB-like factor with a site upstream of the c-myc promoter. Proc. Natl. Acad. Sci. USA **87:**4727–4731.
12. **Frantz, B., E. C. Nordby, G. Bren, N. Steffan, C. V. Paya, R. L. Kincaid, M. J. Tocci, S. J. O'Keefe, and E. A. O'Neill.** 1994. Calcineurin acts in synergy with PMA to inactivate IκB/MAD3, an inhibitor of NF-κB. EMBO J. **13:**861–870.
13. **Ghoda, L., X. Lin, and W. C. Greene.** 1997. The 90-kDa ribosomal S6 kinase (pp90rsk) phosphorylates the N-terminal regulatory domain of IκBα and stimulates its degradation in vitro. J. Biol. Chem. **272:**21281–21288.
14. **Harvey, D. M., and A. J. Levine.** 1991. p53 alteration is a common event in the spontaneous immortalization of primary BALB/c murine embryo fibroblasts. Genes Dev. **5:**2375–2385.
15. **Huang, T. T., S. M. Wuerzberger-Davis, B. J. Seufzer, S. D. Shumway, T. Kurama, D. A. Boothman, and S. Miyamoto.** 2000. NF-κB activation by camptothecin. A linkage between nuclear DNA damage and cytoplasmic signaling events. J. Biol. Chem. **275:**9501–9509.
16. **Hur, G. M., J. Lewis, Q. Yang, Y. Lin, H. Nakano, S. Nedospasov, and Z. G. Liu.** 2003. The death domain kinase RIP has an essential role in DNA damage-induced NF-κB activation. Genes Dev. **17:**873–882.
17. **Kastan, M. B., and D. S. Lim.** 2000. The many substrates and functions of ATM. Nat. Rev. Mol. Cell Biol. **1:**179–186.
18. **Kharbanda, S., P. Pandey, T. Yamauchi, S. Kumar, M. Kaneki, V. Kumar, A. Bharti, Z. M. Yuan, L. Ghanem, A. Rana, R. Weichselbaum, G. Johnson, and D. Kufe.** 2000. Activation of MEK kinase 1 by the c-Abl protein tyrosine kinase in response to DNA damage. Mol. Cell. Biol. **20:**4979–4989.
19. **Kharbanda, S., A. Saleem, T. Shafman, Y. Emoto, R. Weichselbaum, and D. Kufe.** 1994. Activation of the pp90rsk and mitogen-activated serine/threonine protein kinases by ionizing radiation. Proc. Natl. Acad. Sci. USA **91:**5416–5420.
20. **Kharbanda, S., Z. M. Yuan, R. Weichselbaum, and D. Kufe.** 1998. Determination of cell fate by c-Abl activation in the response to DNA damage. Oncogene **17:**3309–3318.
21. **Kim, S. T., D. S. Lim, C. E. Canman, and M. B. Kastan.** 1999. Substrate specificities and identification of putative substrates of ATM kinase family members. J. Biol. Chem. **274:**37538–37543.
22. **Kurimasa, A., S. Kumano, N. V. Boubnov, M. D. Story, C. S. Tung, S. R. Peterson, and D. J. Chen.** 1999. Requirement for the kinase activity of human DNA-dependent protein kinase catalytic subunit in DNA strand break rejoining. Mol. Cell. Biol. **19:**3877–3884.
23. **Lee, S. A., A. Dritschilo, and M. Jung.** 1998. Impaired ionizing radiation-induced activation of a nuclear signal essential for phosphorylation of c-Jun by dually phosphorylated c-Jun amino-terminal kinases in ataxia telangiectasia fibroblasts. J. Biol. Chem. **273:**32889–32894.
24. **Lee, S. J., A. Dimtchev, M. F. Lavin, A. Dritschilo, and M. Jung.** 1998. A

novel ionizing radiation-induced signaling pathway that activates the transcription factor NF-κB. Oncogene **17:**1821–1826.
25. **Li, J. D., W. Feng, M. Gallup, J. H. Kim, J. Gum, Y. Kim, and C. Basbaum.** 1998. Activation of NF-κB via a Src-dependent Ras-MAPK-pp90rsk pathway is required for *Pseudomonas aeruginosa*-induced mucin overproduction in epithelial cells. Proc. Natl. Acad. Sci. USA **95:**5718–5723.
26. **Li, N., S. Banin, H. Ouyang, G. C. Li, G. Courtois, Y. Shiloh, M. Karin, and G. Rotman.** 2001. ATM is required for IκB kinase (IKKk) activation in response to DNA double strand breaks. J. Biol. Chem. **276:**8898–8903.
27. **Lin, R., P. Beauparlant, C. Makris, S. Meloche, and J. Hiscott.** 1996. Phosphorylation of IκBα in the C-terminal PEST domain by casein kinase II affects intrinsic protein stability. Mol. Cell. Biol. **16:**1401–1409.
28. **Lothstein, L., D. P. Suttle, J. F. Roaten, Y. Koseki, M. Israel, and T. W. Sweatman.** 2000. Catalytic inhibition of DNA topoisomerase II by N-benzyladriamycin (AD 288). Biochem. Pharmacol. **60:**1621–1628.
29. **Lothstein, L., H. M. Wright, T. W. Sweatman, and M. Israel.** 1992. N-benzyladriamycin-14-valerate and drug resistance: correlation of anthracycline structural modification with intracellular accumulation and distribution in multidrug resistant cells. Oncol. Res. **4:**341–347.
30. **Lowe, S. W., H. E. Ruley, T. Jacks, and D. E. Housman.** 1993. p53-dependent apoptosis modulates the cytotoxicity of anticancer agents. Cell **74:**957–967.
31. **Mayo, M. W., and A. S. Baldwin.** 2000. The transcription factor NF-κB: control of oncogenesis and cancer therapy resistance. Biochim. Biophys. Acta **1470:**M55–M62.
32. **Mercurio, F., and A. M. Manning.** 1999. Multiple signals converging on NF-κB. Curr. Opin. Cell Biol. **11:**226–232.
33. **Mercurio, F., B. W. Murray, A. Shevchenko, B. L. Bennett, D. B. Young, J. W. Li, G. Pascual, A. Motiwala, H. Zhu, M. Mann, and A. M. Manning.** 1999. IκB kinase (IKK)-associated protein 1, a common component of the heterogeneous IKK complex. Mol. Cell. Biol. **19:**1526–1538.
34. **Mercurio, F., H. Zhu, B. W. Murray, A. Shevchenko, B. L. Bennett, J. Li, D. B. Young, M. Barbosa, M. Mann, A. Manning, and A. Rao.** 1997. IKK-1 and IKK-2: cytokine-activated IκB kinases essential for NF-κB activation. Science **278:**860–866.
35. **Murnane, J. P., L. F. Fuller, and R. B. Painter.** 1985. Establishment and characterization of a permanent pSV ori-transformed ataxia-telangiectasia cell line. Exp. Cell Res. **158:**119–126.
36. **Peterson, S. R., A. Kurimasa, M. Oshimura, W. S. Dynan, E. M. Bradbury, and D. J. Chen.** 1995. Loss of the catalytic subunit of the DNA-dependent protein kinase in DNA double-strand-break-repair mutant mammalian cells. Proc. Natl. Acad. Sci. USA **92:**3171–3174.
37. **Piret, B., and J. Piette.** 1996. Topoisomerase poisons activate the transcription factor NF-κB in ACH-2 and CEM cells. Nucleic Acids Res. **24:**4242–4248.
38. **Piret, B., S. Schoonbroodt, and J. Piette.** 1999. The ATM protein is required for sustained activation of NF-κB following DNA damage. Oncogene **18:**2261–2271.
39. **Pommier, Y., F. Leteurtre, M. R. Fesen, A. Fujimori, R. Bertrand, E. Solary, G. Kohlhagen, and K. W. Kohn.** 1994. Cellular determinants of sensitivity and resistance to DNA topoisomerase inhibitors. Cancer Investig. **12:**530–542.
40. **Reed, J. C., T. Miyashita, S. Takayama, H. G. Wang, T. Sato, S. Krajewski, C. Aime-Sempe, S. Bodrug, S. Kitada, and M. Hanada.** 1996. BCL-2 family proteins: regulators of cell death involved in the pathogenesis of cancer and resistance to therapy. J. Cell. Biochem. **60:**23–32.
41. **Ryan, K. M., M. K. Ernst, N. R. Rice, and K. H. Vousden.** 2000. Role of NF-κB in p53-mediated programmed cell death. Nature **404:**892–897.
42. **Saeki, Y., C. Fraefel, T. Ichikawa, X. O. Breakefield, and E. A. Chiocca.** 2001. Improved helper virus-free packaging system for HSV amplicon vectors using an ICP27-deleted, oversized HSV-1 DNA in a bacterial artificial chromosome. Mol. Ther. **3:**591–601.
43. **Sarkaria, J. N., E. C. Busby, R. S. Tibbetts, P. Roos, Y. Taya, L. M. Karnitz, and R. T. Abraham.** 1999. Inhibition of ATM and ATR kinase activities by the radiosensitizing agent caffeine. Cancer Res. **59:**4375–4382.
44. **Sarkaria, J. N., R. S. Tibbetts, E. C. Busby, A. P. Kennedy, D. E. Hill, and R. T. Abraham.** 1998. Inhibition of phosphoinositide 3-kinase related kinases by the radiosensitizing agent wortmannin. Cancer Res. **58:**4375–4382.
45. **Schouten, G. J., A. C. Vertegaal, S. T. Whiteside, A. Israel, M. Toebes, J. C. Dorsman, A. J. van der Eb, and A. Zantema.** 1997. IκB alpha is a target for the mitogen-activated 90 kDa ribosomal S6 kinase. EMBO J. **16:**3133–3144.
46. **Shafman, T. D., A. Saleem, J. Kyriakis, R. Weichselbaum, S. Kharbanda, and D. W. Kufe.** 1995. Defective induction of stress-activated protein kinase activity in ataxia-telangiectasia cells exposed to ionizing radiation. Cancer Res. **55:**3242–3245.
47. **Shiloh, Y., and M. B. Kastan.** 2001. ATM: genome stability, neuronal development, and cancer cross paths. Adv. Cancer Res. **83:**209–254.
48. **Tang, D., D. Wu, A. Hirao, J. M. Lahti, L. Liu, B. Mazza, V. J. Kidd, T. W. Mak, and A. J. Ingram.** 2002. ERK activation mediates cell cycle arrest and apoptosis after DNA damage independently of p53. J. Biol. Chem. **277:**12710–12717.
49. **Tergaonkar, V., M. Pando, O. Vafa, G. Wahl, and I. Verma.** 2002. p53 stabilization is decreased upon NFκB activation: a role for NFκB in acquisition of resistance to chemotherapy. Cancer Cell **1:**493–503.
50. **Vertegaal, A. C., H. B. Kuiperij, S. Yamaoka, G. Courtois, A. J. van der Eb, and A. Zantema.** 2000. Protein kinase C-alpha is an upstream activator of the IκB kinase complex in the TPA signal transduction pathway to NF-κB in U2OS cells. Cell. Signal. **12:**759–768.
51. **Wang, C. Y., J. C. Cusack, Jr., R. Liu, and A. S. Baldwin, Jr.** 1999. Control of inducible chemoresistance: enhanced anti-tumor therapy through increased apoptosis by inhibition of NF-κB. Nat. Med. **5:**412–417.
52. **Wang, C. Y., D. C. Guttridge, M. W. Mayo, and A. S. Baldwin, Jr.** 1999. NF-κB induces expression of the Bcl-2 homologue A1/Bfl-1 to preferentially suppress chemotherapy-induced apoptosis. Mol. Cell. Biol. **19:**5923–5929.
53. **Wang, X., C. H. McGowan, M. Zhao, L. He, J. S. Downey, C. Fearns, Y. Wang, S. Huang, and J. Han.** 2000. Involvement of the MKK6-p38γ cascade in gamma-radiation-induced cell cycle arrest. Mol. Cell. Biol. **20:**4543–4552.
54. **Xie, J., M. Aszterbaum, X. Zhang, J. M. Bonifas, C. Zachary, E. Epstein, and F. McCormick.** 2001. A role of PDGFRα in basal cell carcinoma proliferation. Proc. Natl. Acad. Sci. USA **98:**9255–9259.
55. **Zambetti, G. P., R. S. Quartin, J. Martinez, I. Georgoff, J. Momand, D. Dittmer, C. A. Finlay, and A. J. Levine.** 1991. Regulation of transformation and the cell cycle by p53. Cold Spring Harbor Symp. Quant. Biol. **56:**219–225.